Clin Transl Imaging (2017) 5:121–133
DOI 10.1007/s40336-016-0209-4

REVIEW ARTICLE

Emerging PET/MRI applications in neuroradiology and neuroscience

Seyed Ali Nabavizadeh[1] · Ilya Nasrallah[1] · Jacob Dubroff[1]

Received: 7 June 2016 / Accepted: 15 September 2016 / Published online: 11 October 2016

Abstract PET and MRI are powerful imaging techniques that have been used extensively to study diseases of the brain, head, and neck. In many diseases, including dementia, epilepsy and head and neck cancers, PET and MRI play important and complementary roles in standard diagnostic evaluation. Recent advances in PET detector technology have allowed combination of PET and MRI into a single machine capable of simultaneous imaging which may offer several, distinct advantages over serial imaging and post-acquisition fusion such as decreased patient burden and improved PET imaging quantification. In addition, a PET/MR instrument potentially has the unique ability to combine time-dependent physiological and functional information from MRI with the specific metabolic and receptor specific information from PET imaging. Over the past several years, numerous anecdotal reports and several larger studies showed the feasibility of PET/MR in various brain and head and neck applications including, for example, concomitant fMRI and PET neuroreceptor imaging. Future well-designed studies with a focus on evaluating and optimizing the synergistic qualities of these combined technologies may fulfill the promise of PET-MRI to provide unparalleled opportunities to understand complex brain function and pathology.

Keywords PET/MR · Neuroimaging · Neuroscience

✉ Jacob Dubroff
Jacob.Dubroff@uphs.upenn.edu

[1] Department of Radiology, Hospital of University of Pennsylvania, Perelman School of Medicine of the University of Pennsylvania, Philadelphia, PA, USA

Introduction

PET and MRI are established clinical and research imaging modalities that provide complementary information by combining excellent soft tissue contrast and temporal resolution of MRI and high sensitivity and molecular specificity of PET. For some applications, primarily in research, it has proven useful to combine them in a post hoc fashion. Such a strategy may be sufficient for many purposes in brain imaging, given the rigid structure of the skull that allows straightforward image registration. Post hoc registration is more challenging in the head and neck. Only recently have technological advances allowed simultaneous MRI and PET imaging, opening up new opportunities for clinical and research neuroimaging. These potential benefits range from improved patient comfort to improved quality of PET data to novel acquisition of time-dependent multi-parametric PET and MRI data to provide new insights into complex processes. The diagnostic and scientific advantages of simultaneous acquisition over post hoc registration have not yet been conclusively established and will likely be limited to select applications. In this review, we describe the methodological and technical aspects of simultaneous PET/MR as well as discuss clinical applications in select brain and head and neck pathologies. Clinical case examples (Figs. 1, 2, 3, 4, 5) are used to support the PET/MR discussion.

Methodological-technical aspects of PET/MR

Since small animal simultaneous PET/MR imaging was initially proposed and performed approximately 20 years ago [1, 2], a decade of work was needed to develop the first simultaneous PET/MR of the brain [3]. In contrast to

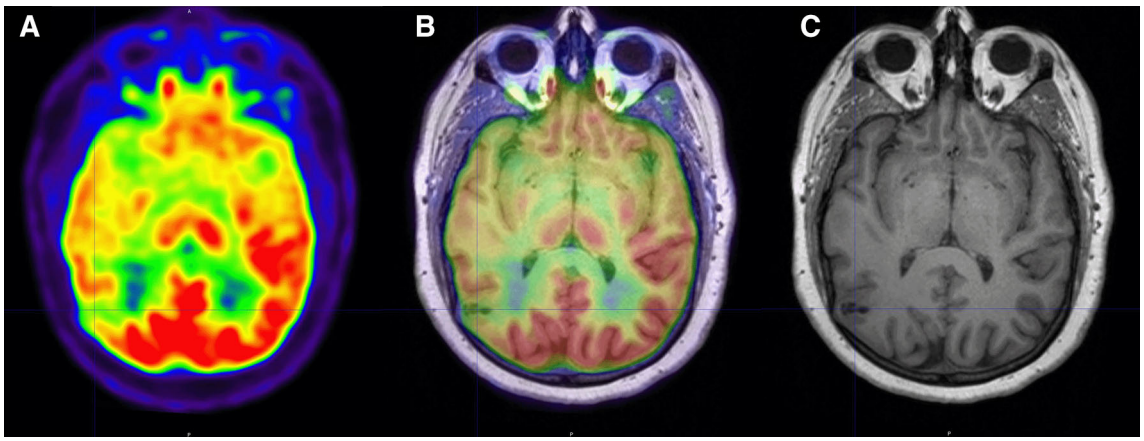

Fig. 1 36-year-old male with intractable seizures who underwent imaging for surgical resection consideration. Crosshairs localize a *right* temporal lesion that appears hypometabolic on ^{18}F-FDG PET (**a**), partially cystic on T1-MRI (**c**). Fused PET/MR images show excellent co-localization (**b**). Morphologically, the lesion was favored to present a dysembryoplastic neuroepithelial tumor (DNET) or ganglioglioma with mild associated cortical dysplasia. Hypometabolism of the lesion and the ipsilateral temporal lobe on ^{18}F-FDG PET was consistent with a right-sided seizure onset

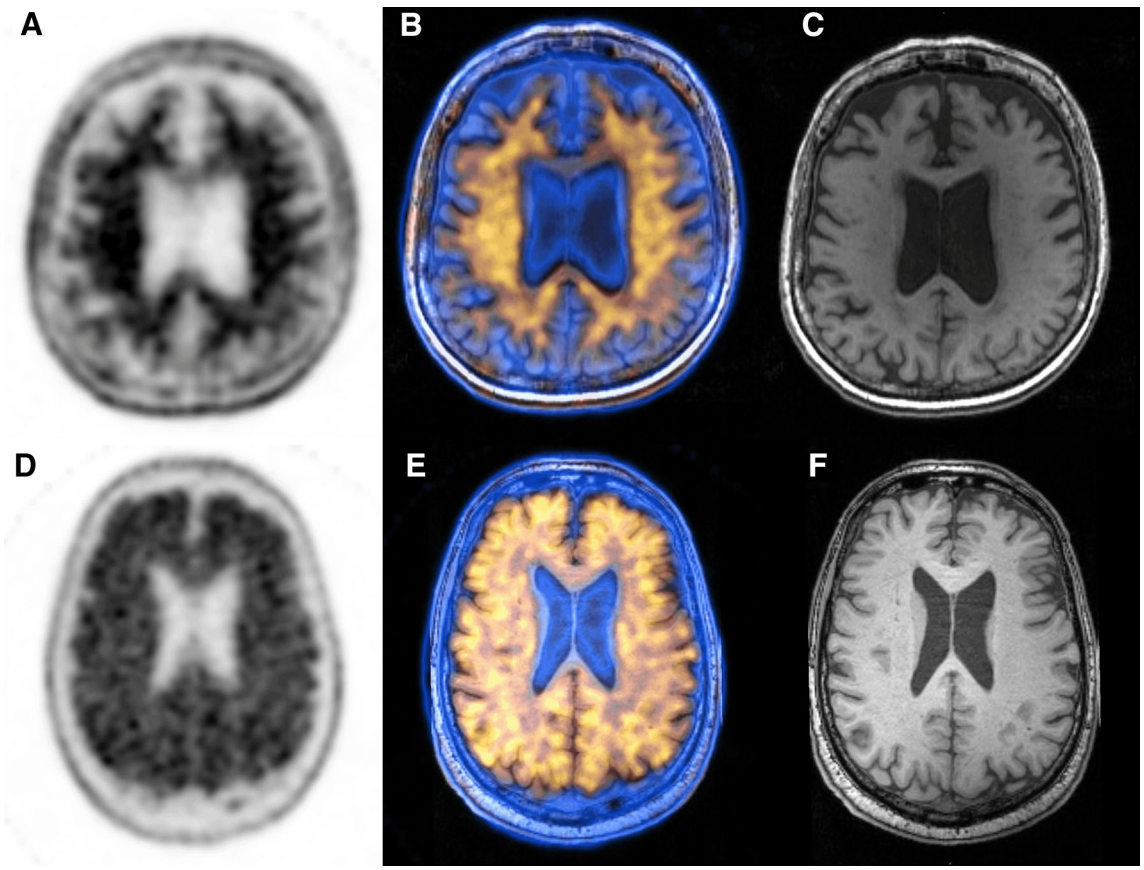

Fig. 2 ^{18}F-florbetapir PET (**a**, **d**), T1-MRI (**c**, **f**), and fusion PET/MR (**b**, **e**) brain imaging in a 70-year-old female (*top row*) and an 88 male (*bottom row*) participating in a research study. The *top row* demonstrates a negative study without significant tracer distribution involving cortical *gray* matter. The *bottom row* shows a positive study in which tracer uptake across the *gray* and *white* matter appears homogenous. Fusion images may permit greater ability to determine abnormal tracer accumulation in the cerebral cortex, especially in patients with significant brain atrophy

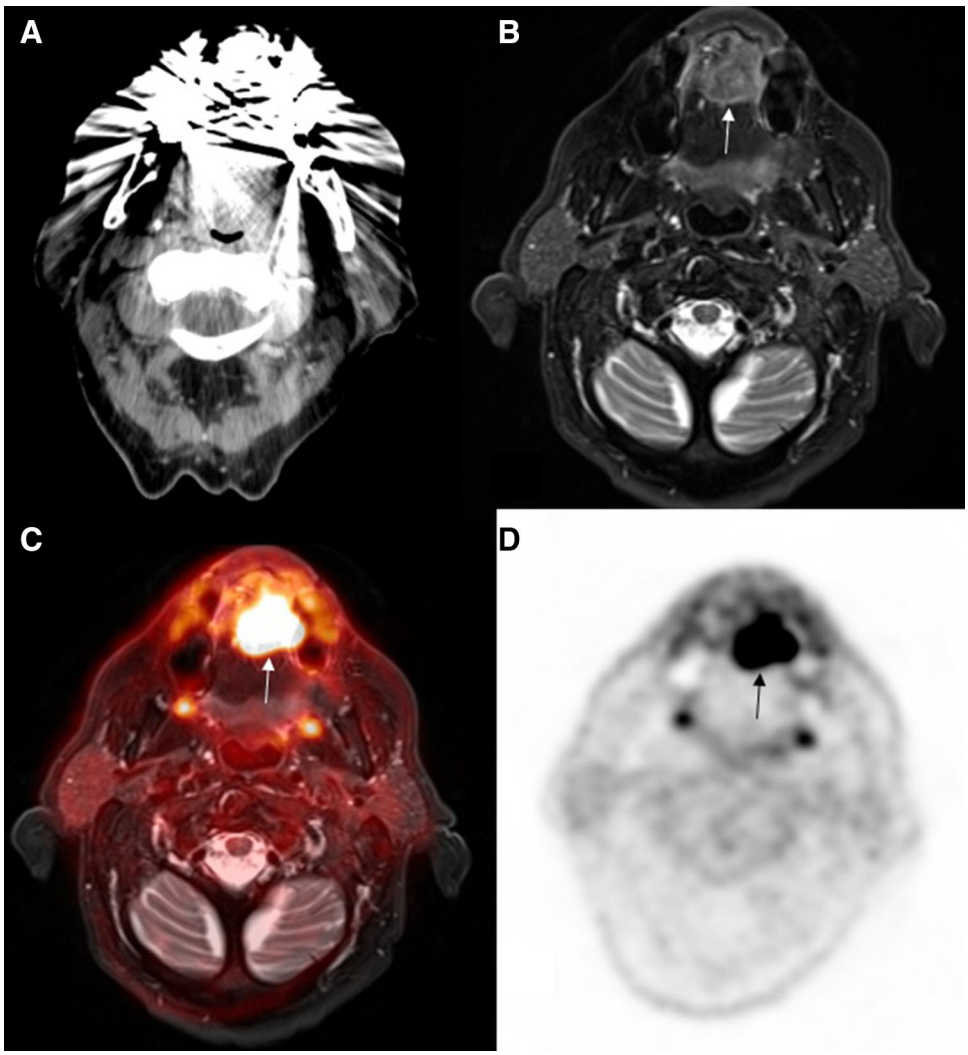

Fig. 3 65-year-old patient with history of a tongue mass. Axial CT scan (**a**) is markedly degraded due to metallic artifact. Axial T2 weighted fat-suppressed MRI clearly demonstrates a hyperintense mass in anterior tongue crossing the midline (**b**, *arrow*). Axial PET/MR and PET images demonstrate marked increased FDG uptake in the mass (**c** and **d**, *arrow*)

integrated PET/CT, where there is no interference between sequentially performed PET and CT imaging, there are several technical challenges in designing an integrated PET/MR machine. For example, standard PET imaging uses an analog photomultiplier tube (PMT) to amplify and detect events using an electron cascade that cannot operate in the high magnetic field in or even near an MRI scanner [4]. In addition, traditional MRI head or surface coils may attenuate PET photons before they can be detected. Finally, the presence of PET detectors, which are placed within the MR gradient coils can interfere with the homogenous magnetic field and gradient function which are required for optimal MR image quality [5].

As typical with new technology, vendors have developed various solutions to solve the technical challenges of PET/MR [6]. A simple approach was to use standalone PET and MRI machines in a serial configuration: Philips' Ingenuity TF system (Philip's Healthcare, Andover, MA) [7, 8] and General Electric's Discovery PET/CT + MR (GE Healthcare, Chicago, IL) [9] are two examples of this approach. Although these systems can provide PET-MRI imaging and are able to utilize state of the art, established hardware for both PET and MRI acquisition, they are limited to sequential imaging. This, in turn, translates into extended acquisition time and a narrow improvement over well-established and rapid post hoc methods of co-registering PET and MRI [2]. In a study of 221 patients using sequential PET-MR imaging, the total examination time ranged up to 2.46 and 3.08 h for brain and head and neck, respectively [10], with half of the unit idle at any time during the study. Sequential PET/MR would need to have a significant diagnostic advantage to justify the utilization in comparison to standalone PET/CT and MRI.

Several significant design and hardware modifications were required to achieve simultaneous PET/MR image acquisition. PMTs have been replaced by solid-state photodetector devices with radiofrequency shielding to protect from the effects of the magnetic field. Avalanche

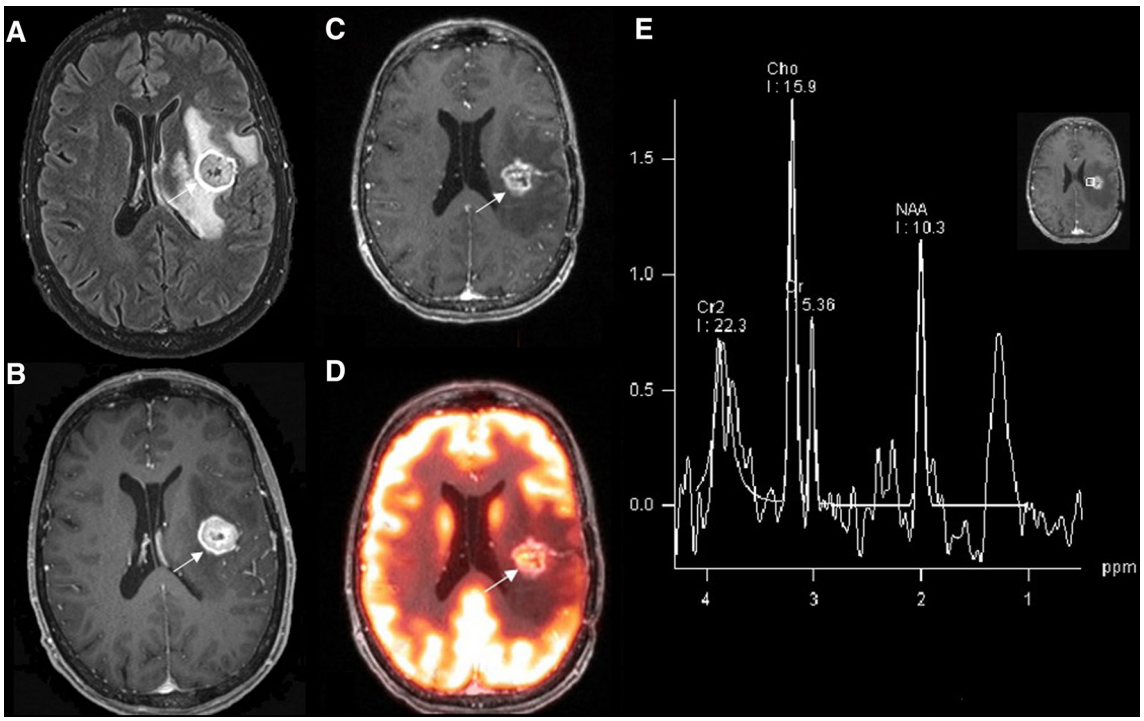

Fig. 4 52-year-old patient with breast cancer metastatic to *left* frontal lobe (**a**, **b**, *arrow*), status post resection of *left* frontal mass followed by Gamma knife radiosurgery to the resection bed. Follow-up imaging demonstrated a heterogeneously enhancing mass is the resection bed (**c**, *arrow*) with elevated ^{18}F-FDG uptake on fused PET/MR image (**d**) and marked elevation of choline:creatine and choline:*N*-acetylaspartate ratios on MR spectroscopy (**e**). Patient underwent resection with histopathology showing recurrent tumor

photodiodes (APD) are used in Siemens (Erlangen, Germany) Biograph mMR while GE (Chicago, USA) Signa PET/MR employs silicon photomultipliers. The APD have lower temporal resolution which do not allow time-of-flight (TOF) PET imaging, a technology with established advantages in quantitation and sensitivity that is standard in modern PET/CT systems [11]. Silicon photomultipliers have excellent temporal resolution and permit TOF imaging [12]. The need for a wide-bore MR scanner to allow space for PET detectors represents an additional modification [13]; current integrated PET/MR systems uniformly have 60 cm bore diameters.

Imaging considerations for PET and MR

For clinical brain PET imaging, the PET tracer is injected prior to the PET/MR session so a steady state is reached by the time of imaging and to allow for clearance of unbound tracer. For clinical brain PET agents, typical imaging times range from 10 to 20 min [14] performed 30–90 min after tracer injection. These standard clinical PET acquisitions, therefore, reflect the steady state of tracer distribution and binding from 30 to 90 min earlier; simultaneous PET/MR image acquisition does not necessarily ensure that one will evaluate processes occurring at the same time. Compared to PET acquisitions, standard clinical MRI studies are longer, typically 20–30 min. Standard clinical protocols acquire structural MRI sequences such as T1 weighted and FLAIR, which can be used for anatomic correlation, serving one purpose of the unenhanced CT component of a PET/CT scan. Finally, the addition of advanced or investigational MRI pulse sequences such as perfusion imaging, MR spectroscopy (MRS), diffusion tensor imaging (DTI) and functional MRI can significantly further lengthen the MR study.

There are several choices that can be made to reconcile the different time requirements for PET and MRI acquisition. The MRI study could be optimized to match the PET scan length and minimize ‘table time’, either by selecting more rapid sequences that have lower spatial or contrast resolution or by reducing the number of sequences. However, if a separate MRI study is required to gather the remaining data, the convenience benefit of PET/MR is then eliminated. One could use a longer imaging time for continued PET acquisition, permitting injection of lower radiotracer doses and decreasing patient radiation dose. Dynamic PET studies, currently used in research for some radiotracers, on the other hand, often take 60 min and in some cases longer [14].

Imaging in multisite research studies using PET/MR has additional considerations. Standardization of standalone PET and MRI scanners between sites, particularly between

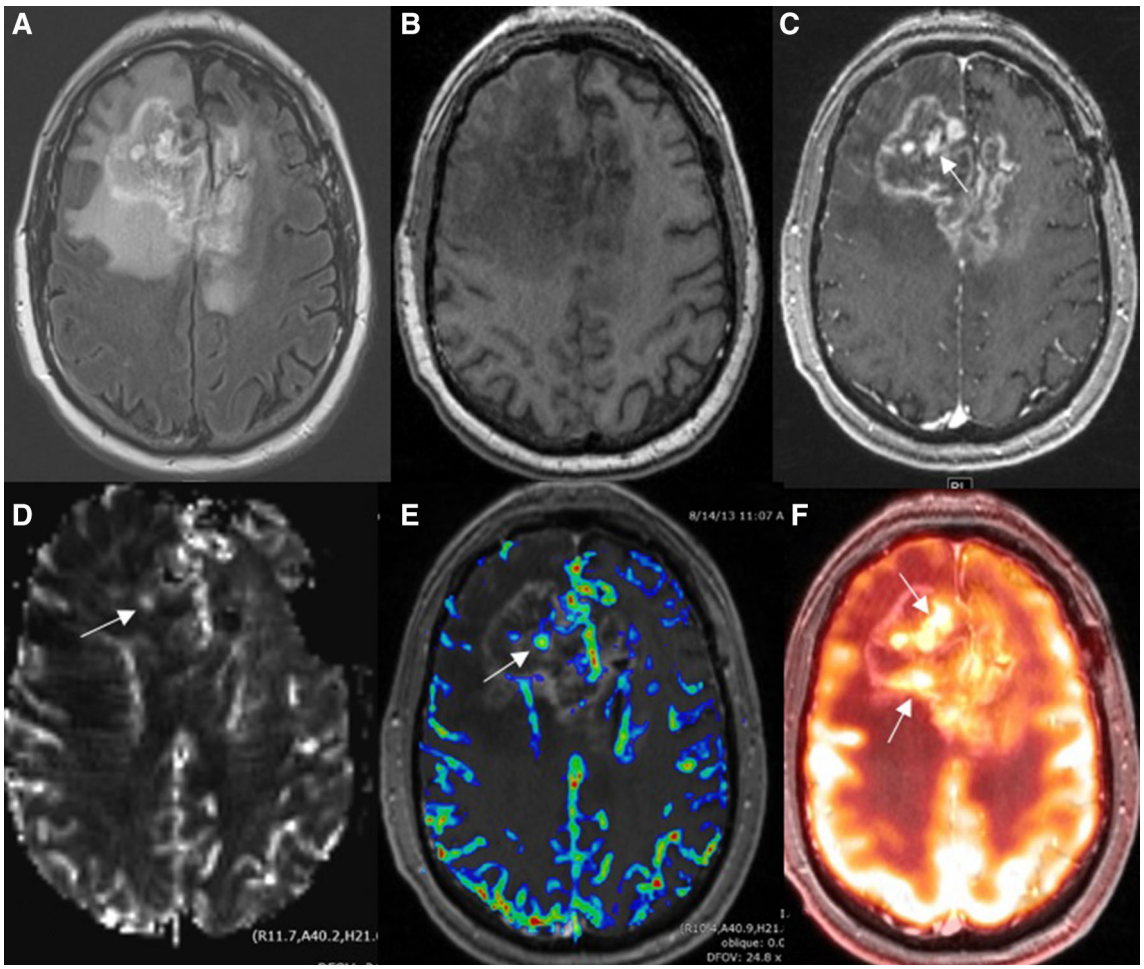

Fig. 5 50-year-old patient, 6 months after debulking and chemoradiation of a bifrontal glioblastoma. Axial FLAIR and axial T1 weighted images demonstrate a bifrontal mass (**a** and **b**) with soap bubble and nodular (**c**, *arrow*) enhancement. DSC perfusion map (**d**) demonstrates a nodular area of increased perfusion that corresponds to nodular enhancement on overlaid perfusion-T1 weighted image (**d** and **e**). Axial PET/MR image demonstrates multiple areas of increased ^{18}F-FDG uptake, some of which do not correspond to increased perfusion (**f**, posterior *arrow*). Patient underwent surgery and histopathology demonstrated mixed tissue with treatment-related changes, with associated viable tumor cells

scanners from different vendors, is challenging due to constraints on imaging parameters and variation in reconstruction. Ensuring uniformity of both PET and MRI data including post-processing on combined PET/MR scanners will likely be even more challenging.

MR-based attenuation correction

Attenuation correction is the process of accounting for the absorption of photons by patient tissues; it is critical for accurate interpretation and quantification of PET data. Historically, there have been two main methods for attenuation correction. For PET-only scanners, attenuation was directly measured using a 511-keV transmission source. When PET/CT was developed, this was replaced by calculating a tissue density attenuation map from the CT acquisition [13] using a relatively straightforward scaling from the low energy of CT to the higher energy of PET.

One of the great challenges of PET/MR development has been to develop methods to estimate photon attenuation using radiofrequency MR imaging, where imaging appearances do not correspond to tissue density. Bone, for example, has the highest natural tissue density in the body but contains few water protons resulting in a very low MR signal, thus appearing similar in intensity to air, which has the lowest density. The most common approach to attenuation correction in PET/MR imaging is using a T1 weighted Dixon sequence to segment the body into up to four classes: air, lung, fat, and soft tissue. Then, a fixed attenuation coefficient is applied to each tissue [15]. The main disadvantage of this method is that bone will be classified as soft tissue and the PET standard uptake value (SUV) of tissues adjacent to bones can erroneously be

underestimated [16] in comparison to SUV values derived from PET/CT. Studies have shown biases typically about 5–10 % with some studies showing bias up to 30 % [17–19].

There are multiple solutions to improve MR-based attenuation correction. One approach available for the brain is to use atlas based information to account for bony structures, however, this method does not accurately capture individual variability in calvarial structure [20]. Another approach is the use of ultrashort TE sequences to generate pseudo-CT images [21], allowing the definition of bone tissue. In addition, TOF PET/MR systems can take advantage of the TOF information to further reduce attenuation correction artifacts [22, 23]. An additional challenge is posed by MR coil devices and the patient table, both of which are invisible to MRI but which cause photon attenuation, requiring correction in post-processing. The complexity of attenuation correction for head and neck or whole body PET/MR is even greater than brain imaging without the benefits of the rigid structure of the calvarium and relative isolation from cardiopulmonary motion.

Metal implants represent another source of signal loss and artifact on MR, which can adversely affect attenuation correction. Newly developed MRI sequences, such as slice encoding for metal artifact correction and multi-acquisition variable-resonance image combination, can be used to compensate for magnetic field distortions resulting from metallic implants [24–26]. This strategy can be particularly useful in PET/MR evaluation in patients with cancers of the oral cavity. TOF technology can also help to reduce the attenuation correction artifacts associated with metallic hardware [27, 28]. Although multiple variables need to be carefully considered for MR-based attenuation correction, MR contrast is not a factor as studies have already revealed a lack of effect of MR contrast agents on PET quantification [29, 30].

Partial volume and motion correction

One limitation of PET imaging has been evaluation of small structures, in large part due to the distance traveled by the emitted positron before the annihilation event, which causes blurring. In many cases, PET radiotracers have known tissue specificity. For example, ^{18}F-FDG has significantly higher uptake in gray matter than white matter. While CT, particularly the low dose CTs used in PET/CT scanners, cannot reliably identify these different tissues, MRI has significantly greater soft tissue contrast. In PET/MR systems, this knowledge of gray and white matter can be used to accurately identify target tissues and correct PET data for tissue volume [31], similar to the correction performed for tissue attenuation.

Decreased spatial resolution of PET, again particularly for small structures, may also result from patient motion. This is usually most evident near the diaphragm, but also affects studies of the brain. Another advantage of simultaneous PET/MR scanners is the potential for real-time motion correction. Since there is no radiation cost to repeated MR imaging, patient motion can be tracked with fast embedded navigator MR sequences which can be used to more precisely determine the anatomic site of the PET emission [32].

PET tracer uptake and quantification using MR information

One of the great advantages of a simultaneous PET/MR scanner is the ability to apply MRI anatomical and physiologic data to improve PET quantification. PET is most often quantified using standardized uptake values (SUV), which is a relatively simple estimate of tracer binding. More precise methods of quantification use information from an arterial input function (AIF), which describes the time course of radiotracer delivery to the brain, to improve the accuracy of PET quantification. Traditionally in dynamic PET brain imaging, determination of the AIF requires arterial blood sampling; an invasive and technically challenging procedure with additional risks [33, 34] that is not applicable in routine clinical practice. High-resolution MR angiography images have been used to calculate image-derived AIFs [34, 35], providing a non-invasive alternative. For example, Su et al. used co-registered high-resolution MRA images to locate petrous portion of internal carotid artery on PET imaging to extract an AIF that showed good agreement with conventional arterial sampling [34] in CBF measurements using ^{15}O-H_2O PET/MR. While the aforementioned AIF studies did relate PET and MR imaging to one another, none were performed on a combined PET/MR instrument, and therefore, essentially use correlations and not simultaneously acquired PET and MR data.

Clinical applications of PET/MR in brain, and neck

PET-MRI in epilepsy

Epilepsy is one of the most common chronic neurologic disorders for patients [36]. Drug-resistant epilepsy, affecting approximately one-third of epileptics, may benefit from neurosurgery to reduce or eliminate seizures and improve quality of life [37]. In these patients, the goal of imaging is to localize brain tissue that is abnormally functioning and provoking seizure activity as a target for surgical

resection. Brain MR is the mainstay of imaging in patients with epilepsy [38], however, 20–30 % of patients with medial temporal lobe epilepsy may not have an identifiable MRI abnormality [39, 40]. ^{18}F-FDG PET may correctly lateralize the seizure focus in 95 % of MRI positive, 69 % of equivocal and 84 % of MRI-negative patients [41]. Given the complementary role of these modalities, both PET and MRI are usually obtained in patients who are being considered for epilepsy surgery. Co-registration of PET with MRI (Fig. 1) has become standard in some institutions and their synergistic value to improve the identification of epileptogenic foci, aid in surgical planning, and effect improved outcome has been shown in several studies [42–44]. There is strong evidence supporting positive post-surgical outcomes in epilepsy patients with negative MR studies but positive ^{18}F-FDG PET ones [45–48]. Single session simultaneous PET/MR in patients with epilepsy, who are frequently young, may decrease patient burden and radiation exposure compared to separate MRI and PET/CT imaging. Several recent studies have shown that PET/MR is effective in epilepsy patients. Grouiller et al. successfully used single-session EEG/PET/(f) MRI in 12 epilepsy patients and demonstrated that all could be performed simultaneously in less than 2 h [49]. Ding et al. used simultaneous PET/MR in in 11 epilepsy patients and 6 controls and demonstrated metabolic abnormalities and asymmetry patterns over 117 brain regions in epilepsy patients as compared to controls [50]. Another study suggests that simultaneous PET/MR may provide improved diagnostic accuracy: in 29 epilepsy patients, simultaneous PET/MR identified new anatomical or functional lesions not identified on previous separate MRI and PET/CT studies in 17 % of subjects [51]. While these data appear promising, the number of patients remain limited and no compelling outcome data has been published suggesting superiority in simultaneous PET/MR.

PET-MRI in neurodegenerative disorders

Neurodegenerative diseases are the leading cause of dementia and disability in the elderly and are predicted to have a growing impact on the society given the aging population [52]. MRI and PET both provide validated imaging biomarkers of Alzheimer's disease (AD), the most common type of dementia [53].

MRI is widely used in the evaluation of patients with cognitive decline and dementia. One primary function of MRI in patients with suspected dementia is to rule out non-neurodegenerative pathologies such as tumors and infarcts. Of all imaging biomarkers for AD, temporal lobe atrophy seen on MRI has been the most studied [54, 55]. Additionally, quantitative analysis of structural MRI, including the temporal lobe and hippocampi, has been shown promising in the diagnosis of early stage AD and for monitoring disease progression [56, 57]. Although further validation studies are necessary, advanced MRI sequences such as arterial spin labeling (ASL), diffusion tensor imaging (DTI) and functional MRI have demonstrated early promise for AD diagnosis. For example, DTI has been found to be useful in the detection of early white matter changes in patients with dementia [58].

On ^{18}F-FDG PET brain imaging, AD is characterized by hypometabolism in parietotemporal lobes, posterior cingulate cortex, and precuneus. ^{18}F-FDG PET imaging has proven to be a clinically useful biomarker for neural integrity, for both determining diagnosis and charting disease progression [59]. More recently, radiotracers targeting amyloid plaque deposition, one of the histopathological hallmarks of AD, have become available for clinical use; these tracers, ^{18}F-florbetaben, ^{18}F-florbetapir, and ^{18}F-flutemetamol, demonstrate a high specificity for distinguishing suspected AD patients from cognitively normal individuals (Fig. 2) [53]. The high sensitivity of PET amyloid imaging suggests that it may have utility in detecting prodromal AD [60, 61]. More recently, several groups have evaluated the potential to use dynamic measurement of these tracers to measure brain perfusion and have found high correlations with patterns of hypometabolism on ^{18}F-FDG PET [62]. Such a technique could provide an alternative biomarker of neuronal integrity and obviate the need for ^{18}F-FDG PET while taking advantage of longer available PET acquisition time in a combined PET-MR.

Given the already highly successful application of PET and MRI individually to basic and clinical neuroscience as well as the complementary information they provide, integrated PET/MR imaging represents an exciting horizon of exploration for AD and dementia biomarkers. Combined biomarkers may allow greater sensitivity and precision of diagnosis, allowing for earlier diagnosis, prediction of conversion to dementia, and monitoring of treatment agents. For example, Shaffer et al. demonstrated that combined MRI, ^{18}F-FDG PET, and CSF biomarkers demonstrated the highest accuracy for predicting conversion to AD in non-demented subjects with early cognitive decline [61]. Integrated PET/MR have the highest potential to impact clinical and research use in dementia by improving sensitivity in early detection, via improved PET quantification and PET-MR biomarker integration, and by allowing novel, simultaneous investigation of molecular events detectable by PET and physiologic brain states measured by MRI. For example, a study of twenty patients with a diagnosis of AD and twenty patients diagnosed with frontotemporal lobar degeneration, another neurodegenerative disease, using integrated ^{18}F-FDG PET/MR imaging demonstrated that these syndromes could be optimally

distinguished using a combination of regional metabolism, functional connectivity, and gray matter volume derived from disease characteristic networks [63]. In a simultaneous PET/MR study examining 24 patients with variants of Alzheimer's disease and frontotemporal dementia, the concordance of atrophy and hypometabolism differed markedly across syndromic variants of Alzheimer's disease and frontotemporal dementia. In addition, quantitative methods identified more widespread atrophy and hypometabolism than qualitative visual ratings reaffirming the implicit but incompletely explored synergy between these two modalities in evaluation of neurological disease [64]. However, the early studies reported thus far have proven that PET/MR can be used in evaluating neurodegeneration but have not taken full advantage of the unique synergies of simultaneous PET/MR acquisition, relying on PET and MRI protocols that could be performed independently.

Integrated PET/MR may also prove beneficial for other neurodegenerative disorders such as Parkinson's disease (PD). Abnormalities of the dopaminergic system that are characteristic of PD can be detected with PET radiotracers such as ^{18}F-DOPA, which has been shown to correlate with symptom severity in patients with PD [65, 66]. Similarly, ^{18}F-(+)fluoropropyl-dihydrotetrabenazine (^{18}F-AV-133), a marker of type 2 vesicular monamine transporter, also correlates well with PD symptom severity [67, 68]. In addition, PET tracers such as ^{11}C-3-amino-4-(2-dimethylaminomethyl-phenylsulfanyl)-benzonitrile (^{11}C-DASB) can evaluate serotonergic system, which can be abnormal in PD [69]. Many of these neurotransmitter radiotracers provide little anatomic detail of the brain, and therefore, benefit from precise tissue localization offered by MRI. Future investigations will likely target the interactions between neuroreceptor biology and brain network function. To that end, Sander and colleagues demonstrated that injection of pharmacologic doses of raclopride was associated with increases in cerebral perfusion and reductions in radiolabeled ^{11}C-raclopride binding in the dopamine-rich striatum [70]. Simultaneous PET/functional MRI provides unique opportunities to temporally relate dynamic and interrelated processes such as these.

PET/MR in neuro-oncology

MRI is by far the modality of choice in evaluation of intracranial neoplasia, primarily due to superior anatomic detail relative to other modalities. Conventional MRI sequences provide high-resolution anatomical images permitting intracranial mass classification, including location, presence of necrosis and blood products, and patterns of enhancement. Nevertheless, these characteristics determined by conventional MRI provide only moderate accuracy in differential diagnosis and in distinguishing recurrence from treatment effects [71]. Advanced MRI techniques such as MR spectroscopy and perfusion MR imaging have modestly improved the diagnostic accuracy by providing additional information about metabolism and vascularity (Fig. 4). However, these techniques also have technical limitations, particularly in the presence of blood products [34, 72, 73] and have suboptimal specificity to differentiate treatment effect from recurrent glioma [73, 74].

While ^{18}F-FDG PET is occasionally used to help differentiate tumor recurrence from radiation necrosis [75], intrinsic intense physiologic uptake by normal gray matter limits its diagnostic accuracy (Fig. 5). However, PET is uniquely able to evaluate metabolic abnormalities of brain neoplasia, including evaluation of amino acid metabolism (^{11}C-methionine, ^{18}F-fluoroethyltyrosine, ^{18}F-DOPA), DNA turnover (^{18}F-fluoro-L-tyrosine [FLT]) and membrane turnover (^{18}F-choline), both elevated in neoplasm and low in the normal brain parenchyma [31, 76]. PET radiotracers targeting hypoxia, such as ^{18}F-fluoromisonidazole (^{18}F-FMISO), also may prove useful in the evaluation of brain neoplasia as a proposed biomarker for resistance to radiotherapy [77]. Combined PET/MR using these tracers may allow for critically needed complementary information without increasing imaging burden on these chronically ill patients, to hopefully provide improved diagnostic and prognostic evaluation over standard MRI.

PET/MR has also been used to guide stereotactic biopsies to the focus of highest tumor grade [78]. A recent study of glioma patients who underwent simultaneous ^{11}C-methionine multi-parametric PET/MR imaging showed that a high level of ^{11}C-methionine uptake, indicative of proliferating tumor cell populations, did not always corresponded to areas of high choline:*N*-acetylaspartate ratio, a marker of proliferation on MR spectroscopy [79]. In a study of 31 glioma patients, Pauleit et al. demonstrated that combination of MRI and ^{18}F-fluoroethyltyrosine PET significantly improves identification of tumor tissue when areas demonstrating both abnormal PET and MRI signals were targeted [80]. Combined PET/MR may allow improved evaluation of the heterogeneity of gliomas and associated treatment effects, particularly given the limitations of established MRI techniques in the setting of immunotherapy [81, 82]. In pediatric patients, where the reduced radiation dose afforded by PET/MR over PET/CT is even more important [82], a study of 12 patients with astrocytomas, using ^{18}F-fluoroethylcholine (^{18}F-choline) PET/MR showed concordance between reduction in tumor size and reductions in ^{18}F-choline uptake [83]. However, other PET/MR studies have shown that each modality can provide complementary information including Henrikson et al. who found heterogeneity of PET and MRI markers of

aggressive neoplasm in 32 glioma patients using ^{18}F-fluoroethyltyrosine PET/MR [84].

PET/MR may also allow for improved quantification of some of these tracers. ^{18}F- fluoro-L-tyrosine is a thymidine analog that becomes trapped in mitotically active cells by thymidine kinase [85], providing a quantitative measure of mitosis. Because uptake of ^{18}F- fluoro-L-tyrosine is limited by blood–brain barrier [86], accurate quantification of DNA synthesis requires complete kinetic modeling of uptake, transport, and metabolism [87]. Given that ability of MRI to evaluate blood–brain barrier permeability, ^{18}F-FLT PET/MR could provide added value beyond either modality alone [31].

PET/MR in head and neck cancer

Imaging of neck and neck cancers using a combined PET/MR instrument represents a promising horizon because of the complementary roles PET and MR individually play in the clinical evaluation of these diseases. MRI is superior to other modalities, including PET and CT, in detecting small but critically important findings in head and neck cancer, including perineural spread and early infiltration of important anatomic structures such as prevertebral fascia and great vessel walls. Contrast-enhanced MR identifies the local extent of a tumor better than does ^{18}F-FDG PET/CT, however, suffers from lack of specificity. ^{18}F-FDG PET/CT is often used in post-treatment follow-up because of its established high negative predictive value for detecting recurrence [88, 89].

Feasibility studies using both sequential and simultaneous image acquisition in patients with head and neck cancers have demonstrated the successful application of PET/MR with excellent imaging quality as well as improved spatial and temporal resolution [90, 91]. There is already evidence that PET/MR performs comparably to PET/CT in local staging and lymph node metastasis [91, 92]. However, there is also preliminary evidence to suggest that contrast-enhanced ^{18}F-FDG PET/MR has higher sensitivity compared to contrast-enhanced ^{18}F-FDG PET/CT in detecting perineural spread [91]. One important consideration in patients with head and neck cancer is the relatively high incidence of distant, systemic metastasis, seen in up to 15 % [93]. Further, head and neck and other aerodigestive tract neoplasms share common risk factors, including smoking and alcohol consumption, resulting in development of second primary neoplasms in up to 10 % of head and neck cancer patients [94]. ^{18}F-FDG PET is routinely used for whole body imaging, adding critical additional data to localized MR studies.

MR provides both opportunities and challenges for attenuation correction. One of the problems commonly encountered in patients with neoplasm of the oral cavity is the presence of dental hardware generating CT artifact. While dental hardware can also generate artifacts on MR, it is often less prominent compared to CT. There are several strategies for artifact reduction in simultaneous PET/MR that have already been successfully implemented (Fig. 3) [28, 95]. On the other hand, unlike in neuroimaging, PET/MR imaging of the head and neck is more vulnerable to motion-related artifacts from respiration and arterial pulsation. Careful planning of MRI acquisition, including orientation of phase-encoding gradients and use of spin-echo sequences to reduce artifacts from arterial pulsation and other physiologic motion and air-tissue interfaces can improve attenuation correction maps [96]. Initial experiences indicate that MR attenuation correction results in comparable lesion detection to PET/CT, although there are differences in SUV quantification [92].

Other potential applications

Neurovascular diseases and stroke Although CT is the most widely used imaging modality for acute stroke imaging, MRI has been increasingly utilized to detect acute ischemia due to higher sensitivity and lack of radiation exposure. MRI has also been used in clinical trials to select patients who will benefit from systemic thrombolysis [97]. Perfusion–diffusion mismatch determined by MR imaging [98] can identify tissues with a critical but reversible decrease in cerebral blood flow. This has been adapted from ^{15}O-H_2O PET imaging, considered the gold standard [99] for quantification of cerebral blood flow measurements. Several MRI techniques are available to measure cerebral perfusion, including dynamic susceptibility-weighted (DSC) and arterial spin labeling (ASL). PET/MR will have a role in validating MR perfusion metrics; simultaneous measurement is essential for optimal cross-validation due to the short time-course of variations in local cerebral perfusion. Two recent studies compared ASL perfusion with ^{15}O-H_2O PET in diabetics and healthy controls. They both demonstrated a good correlation between ASL and ^{15}O-H_2O PET CBF values, but ASL values were less accurate [100, 101]. In another study, using ^{15}O-water PET and ASL in newborn piglets, global ASL cerebral blood flow (CBF) and PET CBF were congruent during baseline but not during hyperperfusion and ASL-derived CBF was questionable for regional blood flow measurements [102].

Measuring brain perfusion using ASL while concomitantly determining hypoxia using tracer such as ^{18}F-fluoromisonidazole PET may be useful in the setting of subarachnoid hemorrhage [103] or cerebral artery vasospasm could be very compelling. However, clinical applications of PET/MR in stroke will be limited by logistic

challenges of maintaining radiotracer availability for unpredictable, acute events.

Multiple sclerosis

Multimodality MR imaging has been the cornerstone of multiple sclerosis imaging and has been used to target different characteristics of disease activity, iron deposition, and white matter changes [104]. Translocator protein (TSPO) PET tracers can identify activated microglia; an increase in TSPO uptake has the potential to act as a biomarker of disease severity and progression in multiple sclerosis [105]. Other radiotracers such as ^{18}F-FDG and ^{18}F-fluoromethylcholine have also used to assess the metabolic changes of multiple sclerosis [106]. A case report also showed the utility of PET/MR to differentiate variants of MS [106], however, large prospective studies are required to determine the value of multimodality PET/MR imaging in demyelinating diseases. Again, these imaging modalities can be fused with one another in a post hoc fashion, so benefits of combined PET/MR in MS would likely primarily depend on efficacy of novel tracers, potential improvement in PET quantification, and lower burden of imaging for patients.

Future directions

Since the introduction of PET/MR to clinical human imaging, the majority of studies comparing PET/MR to PET/CT in brain and head and neck pathologies have used ^{18}F-FDG as the radiotracer and have establishing the feasibility of PET/MR. However, the novel potential of PET/MR lies in combining novel PET probes with multi-parametric MR. Simultaneous PET/MR imaging provides unparalleled opportunities to measure neuroreceptor occupancy with brain activation and connectivity determined by MRI. Wey et al. simultaneously evaluated opioid pathways with PET and brain network activation using fMRI during a pain stimulus using PET/MR to find correlations of pain-induced changes in the thalamus [107]. Others are pushing the limits of both modalities to measure metabolism using time sensitive hyperpolarized MR and PET tracers in brain tumors [108, 109]. These applications will likely provide a better understanding of complex brain pathologies in the era of personalized medicine.

Applications of PET/MR instrumentation could be expanded with the availability of other imaging technologies. Ideally, close proximity to a cyclotron will allow the use of short-lived radiotracers. Although currently this is mainly useful for research applications, some ^{11}C tracers have already found clinical use such as ^{11}C choline for evaluation of prostate cancer recurrence [110]. PET/MR has been combined with other technologies including hyperpolarized MRI, which requires close proximity of a polarizer to the PET/MR because of the extremely short half-life of hyperpolarized agents.

Careful design and implementation of a PET/MR examination requires a joint effort by a skilled multidisciplinary team. Medical physicists are required to develop and implement PET protocols and MR pulse sequences before routine clinical use. Technologists involved in PET-MR must be trained in handling of radioactive pharmaceuticals as well as MR safety and pulse sequence planning, which will likely require the participation of two technologists. Technologists with dual training in both PET and MR are best suited but rare [111]. Interpreting physicians should protocol both modalities for the necessity of additional MR sequences based on the specific pathology and be able to check image quality. Study interpretation requires readers with expertise in both PET and MR. Paralleling the course of instrumentation development, clinical PET/MR interpretation may initially require involvement of separate readers for each modality but will likely evolve into combined expertise.

Conclusion

Simultaneous PET/MR must be more than a simple combination of PET and MRI images to achieve significant clinical and scientific benefit. It offers the opportunity to improve PET quantification and validate novel MR techniques. It also has the potential to further our understanding of relationships between molecular targets quantified by PET and the high anatomic resolution and physiologic data measured by MRI. With the continued development of new PET radiotracer as well as novel MR sequences, PET/MR represents a promising imaging technology that commands the attention of those researchers and clinicians who strive to improve our understanding of basic science and pathophysiology.

Compliance with ethical standards

Conflict of interest The authors, Seyed Ali Nabavizadeh, Ilya Nasrallah, and Jacob Dubroff, all declare no conflict.

References

1. Shao Y et al (1997) Simultaneous PET and MR imaging. Phys Med Biol 42(10):1965–1970
2. Woods RP, Mazziotta JC, Cherry SR (1993) MRI-PET registration with automated algorithm. J Comput Assist Tomogr 17(4):536–546
3. Schlemmer HP et al (2008) Simultaneous MR/PET imaging of the human brain: feasibility study. Radiology 248(3):1028–1035

4. Catana C et al (2006) Simultaneous acquisition of multislice PET and MR images: initial results with a MR-compatible PET scanner. J Nucl Med 47(12):1968–1976
5. von Schulthess GK et al (2013) Clinical positron emission tomography/magnetic resonance imaging applications. Semin Nucl Med 43(1):3–10
6. Delso G, Ter Voert E, Veit-Haibach P (2015) How does PET/MR work? Basic physics for physicians. Abdom Imaging 40(6):1352–1357
7. Garibotto V et al (2013) Clinical applications of hybrid PET/MRI in neuroimaging. Clin Nucl Med 38(1):e13–e18
8. Zaidi H et al (2011) Design and performance evaluation of a whole-body Ingenuity TF PET-MRI system. Phys Med Biol 56(10):3091–3106
9. Veit-Haibach P et al (2013) PET-MR imaging using a tri-modality PET/CT-MR system with a dedicated shuttle in clinical routine. MAGMA 26(1):25–35
10. Vargas MI et al (2013) Approaches for the optimization of MR protocols in clinical hybrid PET/MRI studies. MAGMA 26(1):57–69
11. Surti S et al (2011) Impact of time-of-flight PET on whole-body oncologic studies: a human observer lesion detection and localization study. J Nucl Med 52(5):712–719
12. Yoon HS et al (2012) Initial results of simultaneous PET/MRI experiments with an MRI-compatible silicon photomultiplier PET scanner. J Nucl Med 53(4):608–614
13. Delso G et al (2011) Performance measurements of the Siemens mMR integrated whole-body PET/MR scanner. J Nucl Med 52(12):1914–1922
14. de Galiza Barbosa F, von Schulthess G, Veit-Haibach P (2015) Workflow in simultaneous PET/MRI. Semin Nucl Med 45(4):332–344
15. Martinez-Moller A et al (2009) Tissue classification as a potential approach for attenuation correction in whole-body PET/MRI: evaluation with PET/CT data. J Nucl Med 50(4):520–526
16. Kim JH et al (2012) Comparison of segmentation-based attenuation correction methods for PET/MRI: evaluation of bone and liver standardized uptake value with oncologic PET/CT data. J Nucl Med 53(12):1878–1882
17. Aznar MC et al (2014) Whole-body PET/MRI: the effect of bone attenuation during MR-based attenuation correction in oncology imaging. Eur J Radiol 83(7):1177–1183
18. Samarin A et al (2012) PET/MR imaging of bone lesions–implications for PET quantification from imperfect attenuation correction. Eur J Nucl Med Mol Imaging 39(7):1154–1160
19. Izquierdo-Garcia D, Catana C (2016) MR Imaging–Guided Attenuation Correction of PET Data in PET/MR Imaging. PET Clin 11(2):129–149
20. Hofmann M et al (2011) MRI-based attenuation correction for whole-body PET/MRI: quantitative evaluation of segmentation- and atlas-based methods. J Nucl Med 52(9):1392–1399
21. Delso G et al (2014) Anatomic evaluation of 3-dimensional ultrashort-echo-time bone maps for PET/MR attenuation correction. J Nucl Med 55(5):780–785
22. Boellaard R et al (2014) Accurate PET/MR quantification using time of flight MLAA image reconstruction. Mol Imaging Biol 16(4):469–477
23. Rezaei A, Defrise M, Nuyts J (2014) ML-reconstruction for TOF-PET with simultaneous estimation of the attenuation factors. IEEE Trans Med Imaging 33(7):1563–1572
24. Chen CA et al (2011) New MR imaging methods for metallic implants in the knee: artifact correction and clinical impact. J Magn Reson Imaging 33(5):1121–1127
25. Koch KM et al (2009) A multispectral three-dimensional acquisition technique for imaging near metal implants. Magn Reson Med 61(2):381–390
26. Lu W et al (2009) SEMAC: slice encoding for metal artifact correction in MRI. Magn Reson Med 62(1):66–76
27. Davison H et al (2015) Incorporation of time-of-flight information reduces metal artifacts in simultaneous positron emission tomography/magnetic resonance imaging: a simulation study. Invest Radiol 50(7):423–429
28. Gunzinger JM et al (2014) Metal artifact reduction in patients with dental implants using multispectral three-dimensional data acquisition for hybrid PET/MRI. EJNMMI Phys 1(1):102
29. Lee W et al (2011) Effects of MR contrast agents on PET quantitation in PET-MRI study. J Nucl Med 52(suppl 1):53
30. Lois C et al (2012) Effect of MR contrast agents on quantitative accuracy of PET in combined whole-body PET/MR imaging. Eur J Nucl Med Mol Imaging 39(11):1756–1766
31. Catana C et al (2012) PET/MRI for neurologic applications. J Nucl Med 53(12):1916–1925
32. Catana C et al (2011) MRI-assisted PET motion correction for neurologic studies in an integrated MR-PET scanner. J Nucl Med 52(1):154–161
33. Raichle ME et al (1983) Brain Blood Flow Measured with Intravenous H2150. II. Implementation and validation. J Nucl Med 24(9):790–798
34. Su Y et al (2013) Noninvasive estimation of the arterial input function in positron emission tomography imaging of cerebral blood flow. J Cereb Blood Flow Metab 33(1):115–121
35. Fung EK, Carson RE (2013) Cerebral blood flow with [^{15}O] water PET studies using an image-derived input function and MR-defined carotid centerlines. Phys Med Biol 58(6):1903–1923
36. Kwan P, Brodie MJ (2003) Clinical trials of antiepileptic medications in newly diagnosed patients with epilepsy. Neurology 60(11 Suppl 4):S2–S12
37. Engel Jr J et al (2003) Practice parameter: temporal lobe and localized neocortical resections for epilepsy. Epilepsia 44(6):741–751
38. Jones AL, Cascino GD (2016) Evidence on Use of Neuroimaging for Surgical Treatment of Temporal Lobe Epilepsy: A Systematic Review. JAMA Neurol 73(4):464–470
39. Theodore WH et al (2001) Hippocampal volume and glucose metabolism in temporal lobe epileptic foci. Epilepsia 42(1):130–132
40. Theodore WH et al (1992) Temporal lobectomy for uncontrolled seizures: the role of positron emission tomography. Ann Neurol 32(6):789–794
41. Gok B et al (2013) The evaluation of FDG-PET imaging for epileptogenic focus localization in patients with MRI positive and MRI negative temporal lobe epilepsy. Neuroradiology 55(5):541–550
42. Chassoux F et al (2010) FDG-PET improves surgical outcome in negative MRI Taylor-type focal cortical dysplasias. Neurology 75(24):2168–2175
43. Lee KK, Salamon N (2009) [^{18}F] fluorodeoxyglucose-positron-emission tomography and MR imaging coregistration for presurgical evaluation of medically refractory epilepsy. AJNR Am J Neuroradiol 30(10):1811–1816
44. Salamon N et al (2008) FDG-PET/MRI coregistration improves detection of cortical dysplasia in patients with epilepsy. Neurology 71(20):1594–1601
45. Capraz IY et al (2015) Surgical outcome in patients with MRI-negative, PET-positive temporal lobe epilepsy. Seizure 29:63–68

46. Carne RP et al (2004) MRI-negative PET-positive temporal lobe epilepsy: a distinct surgically remediable syndrome. Brain 127(Pt 10):2276–2285
47. LoPinto-Khoury C et al (2012) Surgical outcome in PET-positive, MRI-negative patients with temporal lobe epilepsy. Epilepsia 53(2):342–348
48. Yang PF et al (2014) Long-term epilepsy surgery outcomes in patients with PET-positive, MRI-negative temporal lobe epilepsy. Epilepsy Behav 41:91–97
49. Grouiller F et al (2015) All-in-one interictal presurgical imaging in patients with epilepsy: single-session EEG/PET/(f) MRI. Eur J Nucl Med Mol Imaging 42(7):1133–1143
50. Ding YS et al (2014) A pilot study in epilepsy patients using simultaneous PET/MR. Am J Nucl Med Mol Imaging 4(5):459–470
51. Shin HW et al (2015) Initial experience in hybrid PET-MRI for evaluation of refractory focal onset epilepsy. Seizure 31:1–4
52. Gaugler J, James B, Johnson T, Scholz K, Weuve J. for the Alzheimer's Association (2014) 2014 Alzheimer's disease facts and figures. Alzheimers Dement 10(2):e47–e92
53. Nasrallah IM, Wolk DA (2014) Multimodality imaging of Alzheimer disease and other neurodegenerative dementias. J Nucl Med 55(12):2003–2011
54. De Leon MJ et al (1993) Measurement of medial temporal lobe atrophy in diagnosis of Alzheimer's disease. Lancet 341(8837):125–126
55. Whitwell JL et al (2008) MRI patterns of atrophy associated with progression to AD in amnestic mild cognitive impairment. Neurology 70(7):512–520
56. Davatzikos C et al (2009) Longitudinal progression of Alzheimer's-like patterns of atrophy in normal older adults: the SPARE-AD index. Brain 132(Pt 8):2026–2035
57. Fan Y et al (2008) Structural and functional biomarkers of prodromal Alzheimer's disease: a high-dimensional pattern classification study. Neuroimage 41(2):277–285
58. Shu N et al (2012) Disrupted topological organization in white matter structural networks in amnestic mild cognitive impairment: relationship to subtype. Radiology 265(2):518–527
59. Choo IH et al (2013) Combination of ^{18}F-FDG PET and cerebrospinal fluid biomarkers as a better predictor of the progression to Alzheimer's disease in mild cognitive impairment patients. J Alzheimers Dis 33(4):929–939
60. Barthel H et al (2011) Cerebral amyloid-beta PET with florbetaben (^{18}F) in patients with Alzheimer's disease and healthy controls: a multicentre phase 2 diagnostic study. Lancet Neurol 10(5):424–435
61. Shaffer JL et al (2013) Predicting cognitive decline in subjects at risk for Alzheimer disease by using combined cerebrospinal fluid, MR imaging, and PET biomarkers. Radiology 266(2):583–591
62. Hsiao IT et al (2012) Correlation of early-phase ^{18}F-florbetapir (AV-45/Amyvid) PET images to FDG images: preliminary studies. Eur J Nucl Med Mol Imaging 39(4):613–620
63. Tahmasian M et al (2016) Based on the network degeneration hypothesis: separating individual patients with different neurodegenerative syndromes in a preliminary hybrid PET/MR study. J Nucl Med 57(3):410–415
64. Moodley KK et al (2015) Simultaneous PET-MRI Studies of the Concordance of Atrophy and Hypometabolism in Syndromic Variants of Alzheimer's Disease and Frontotemporal Dementia: An Extended Case Series. J Alzheimers Dis 46(3):639–653
65. Bruck A et al (2006) Striatal subregional 6-[^{18}F] fluoro-L-dopa uptake in early Parkinson's disease: A two-year follow-up study. Mov Disord 21(7):958–963
66. Pikstra AR et al (2016) Relation of 18-F-Dopa PET with hypokinesia-rigidity, tremor and freezing in Parkinson's disease. Neuroimage Clin 11:68–72
67. Hsiao IT et al (2014) Correlation of Parkinson disease severity and ^{18}F-DTBZ positron emission tomography. JAMA Neurol 71(6):758–766
68. Okamura N et al (2010) In vivo measurement of vesicular monoamine transporter type 2 density in Parkinson disease with ^{18}F-AV-133. J Nucl Med 51(2):223–228
69. Pavese N et al (2012) [^{18}F] FDOPA uptake in the raphe nuclei complex reflects serotonin transporter availability. A combined [^{18}F] FDOPA and [11 C] DASB PET study in Parkinson's disease. Neuroimage 59(2):1080–1084
70. Sander CY et al (2013) Neurovascular coupling to D2/D3 dopamine receptor occupancy using simultaneous PET/functional MRI. Proc Natl Acad Sci U S A 110(27):11169–11174
71. Law M et al (2003) Glioma grading: sensitivity, specificity, and predictive values of perfusion MR imaging and proton MR spectroscopic imaging compared with conventional MR imaging. AJNR Am J Neuroradiol 24(10):1989–1998
72. Provenzale JM, Mukundan S, Barboriak DP (2006) Diffusion-weighted and perfusion MR imaging for brain tumor characterization and assessment of treatment response. Radiology 239(3):632–649
73. Wang S et al (2016) Differentiating tumor progression from pseudoprogression in patients with glioblastomas using diffusion tensor imaging and dynamic susceptibility contrast MRI. AJNR Am J Neuroradiol 37(1):28–36
74. Suh CH et al (2013) Prediction of pseudoprogression in patients with glioblastomas using the initial and final area under the curves ratio derived from dynamic contrast-enhanced T1-weighted perfusion MR imaging. AJNR Am J Neuroradiol 34(12):2278–2286
75. Hustinx R et al (2005) PET imaging for differentiating recurrent brain tumor from radiation necrosis. Radiol Clin N Am 43(1):35–47
76. Werner P et al (2015) Current status and future role of brain PET/MRI in clinical and research settings. Eur J Nucl Med Mol Imaging 42(3):512–526
77. O'Connor JP et al (2008) Quantitative imaging biomarkers in the clinical development of targeted therapeutics: current and future perspectives. Lancet Oncol 9(8):766–776
78. Asselin MC et al (2012) Quantifying heterogeneity in human tumours using MRI and PET. Eur J Cancer 48(4):447–455
79. Bisdas S et al (2013) Metabolic mapping of gliomas using hybrid MR-PET imaging: feasibility of the method and spatial distribution of metabolic changes. Invest Radiol 48(5):295–301
80. Pauleit D et al (2005) O-(2-[^{18}F]fluoroethyl)-L-tyrosine PET combined with MRI improves the diagnostic assessment of cerebral gliomas. Brain 128(Pt 3):678–687
81. Huang RY et al (2015) Pitfalls in the neuroimaging of glioblastoma in the era of antiangiogenic and immuno/targeted therapy–detecting illusive disease, defining response. Front Neurol 6:33
82. Preuss M et al (2014) Integrated PET/MRI for planning navigated biopsies in pediatric brain tumors. Childs Nerv Syst 30(8):1399–1403
83. Fraioli F et al (2015) ^{18}F-fluoroethylcholine (^{18}F-Cho) PET/MRI functional parameters in pediatric astrocytic brain tumors. Clin Nucl Med 40(1):e40–e45
84. Henriksen OM et al (2016) Simultaneous evaluation of brain tumour metabolism, structure and blood volume using [^{18}F]-fluoroethyltyrosine (FET) PET/MRI: feasibility, agreement and initial experience. Eur J Nucl Med Mol Imaging 43(1):103–112

85. Shields AF et al (1998) Imaging proliferation in vivo with [F-18] FLT and positron emission tomography. Nat Med 4(11):1334–1336
86. Muzi M et al (2006) Kinetic analysis of 3'-deoxy-3'-^{18}F-fluorothymidine in patients with gliomas. J Nucl Med 47(10):1612–1621
87. Ullrich R et al (2008) Glioma proliferation as assessed by 3'-fluoro-3'-deoxy-L-thymidine positron emission tomography in patients with newly diagnosed high-grade glioma. Clin Cancer Res 14(7):2049–2055
88. Abgral R et al (2009) Does ^{18}F-FDG PET/CT improve the detection of posttreatment recurrence of head and neck squamous cell carcinoma in patients negative for disease on clinical follow-up? J Nucl Med 50(1):24–29
89. Queiroz MA, Huellner MW (2015) PET/MR in cancers of the head and neck. Semin Nucl Med 45(3):248–265
90. Boss A et al (2011) Feasibility of simultaneous PET/MR imaging in the head and upper neck area. Eur Radiol 21(7):1439–1446
91. Kuhn FP et al (2014) Contrast-enhanced PET/MR imaging versus contrast-enhanced PET/CT in head and neck cancer: how much MR information is needed? J Nucl Med 55(4):551–558
92. Varoquaux A et al (2014) Detection and quantification of focal uptake in head and neck tumours: ^{18}F-FDG PET/MR versus PET/CT. Eur J Nucl Med Mol Imaging 41(3):462–475
93. de Bree R et al (2000) Screening for distant metastases in patients with head and neck cancer. Laryngoscope 110(3 Pt 1):397–401
94. Strobel K et al (2009) Head and neck squamous cell carcinoma (HNSCC)–detection of synchronous primaries with ^{18}F-FDG-PET/CT. Eur J Nucl Med Mol Imaging 36(6):919–927
95. Ladefoged CN et al (2015) Dental artifacts in the head and neck region: implications for Dixon-based attenuation correction in PET/MR. EJNMMI Phys 2(1):8
96. Becker M et al (2008) Neoplastic invasion of Laryngeal Cartilage: Reassessment of Criteria for Diagnosis at MR Imaging. Radiology 249(2):551–559
97. Hacke W et al (2008) Thrombolysis with alteplase 3 to 4.5 hours after acute ischemic stroke. N Engl J Med 359(13):1317–1329
98. Thijs VN et al (2001) Relationship between severity of MR perfusion deficit and DWI lesion evolution. Neurology 57(7):1205–1211
99. Heiss WD et al (1998) Tissue at risk of infarction rescued by early reperfusion: a positron emission tomography study in systemic recombinant tissue plasminogen activator thrombolysis of acute stroke. J Cereb Blood Flow Metab 18(12):1298–1307
100. van Golen LW et al (2014) Quantification of cerebral blood flow in healthy volunteers and type 1 diabetic patients: Comparison of MRI arterial spin labeling and [^{15}O] H_2O positron emission tomography (PET). J Magn Reson Imaging 40(6):1300–1309
101. Zhang K et al (2014) Comparison of cerebral blood flow acquired by simultaneous [^{15}O]water positron emission tomography and arterial spin labeling magnetic resonance imaging. J Cereb Blood Flow Metab 34(8):1373–1380
102. Andersen JB et al (2015) Positron emission tomography/magnetic resonance hybrid scanner imaging of cerebral blood flow using 15O-water positron emission tomography and arterial spin labeling magnetic resonance imaging in newborn piglets. J Cereb Blood Flow Metab 35(11):1703–1710
103. Sarrafzadeh AS et al (2010) Imaging of hypoxic–ischemic penumbra with ^{18}F-fluoromisonidazole PET/CT and measurement of related cerebral metabolism in aneurysmal subarachnoid hemorrhage. J Cereb Blood Flow Metab 30(1):36–45
104. Poloni G et al (2011) Recent developments in imaging of multiple sclerosis. Neurologist 17(4):185–204
105. Hagens M, van Berckel B, Barkhof F (2016) Novel MRI and PET markers of neuroinflammation in multiple sclerosis. Curr Opin Neurol 29(3):229–236
106. Bolcaen J et al (2013) Structural and metabolic features of two different variants of multiple sclerosis: a PET/MRI study. J Neuroimaging 23(3):431–436
107. Wey HY et al (2014) Simultaneous fMRI-PET of the opioidergic pain system in human brain. Neuroimage 102(Pt 2):275–282
108. Gutte H et al (2015) Simultaneous hyperpolarized 13C-pyruvate MRI and 18F-FDG PET (HyperPET) in 10 dogs with cancer. J Nucl Med 56(11):1786–1792
109. Keshari KR et al (2015) Metabolic response of prostate cancer to nicotinamide phophoribosyltransferase inhibition in a hyperpolarized MR/PET compatible bioreactor. Prostate 75(14):1601–1609
110. Incerti E et al (2015) Radiation treatment of lymph node recurrence from prostate cancer: is 11C-choline PET/CT predictive of survival outcomes? J Nucl Med 56(12):1836–1842
111. Bolus NE et al (2009) PET/MRI: the blended-modality choice of the future? J Nucl Med Technol 37(2):63–71